



Universidade de São Paulo

Biblioteca Digital da Produção Intelectual - BDPI

Departamento de Engenharia Aeronáutica - EESC/SAA

Artigos e Materiais de Revistas Científicas - EESC/SAA

2012

Effective properties evaluation for smart composite materials

J. Braz. Soc. Mech. Sci. & Eng.,v.34,n.spe,p.362-370,2012

<http://www.producao.usp.br/handle/BDPI/40137>

Downloaded from: Biblioteca Digital da Produção Intelectual - BDPI, Universidade de São Paulo

Ricardo de Medeiros

medeiros@sc.usp.br
 University of São Paulo
 Engineering School of São Carlos
 Department of Aeronautical Engineering
 13563-120 São Carlos, SP, Brazil

Mariano E. Moreno

mmoreno@ufscar.br
 Federal University of São Carlos
 Center of Exact Sciences and Technology
 13565-905 São Carlos, SP, Brazil

Flávio D. Marques

fmarques@sc.usp.br
 University of São Paulo
 Engineering School of São Carlos
 Department of Aeronautical Engineering
 13563-120 São Carlos, SP, Brazil

Volnei Tita

voltita@sc.usp.br
 University of São Paulo
 Engineering School of São Carlos
 Department of Aeronautical Engineering
 13563-120 São Carlos, SP, Brazil

Effective Properties Evaluation for Smart Composite Materials

The purpose of this article is to present a method which consists in the development of unit cell numerical models for smart composite materials with piezoelectric fibers made of PZT embedded in a non-piezoelectric matrix (epoxy resin). This method evaluates a globally homogeneous medium equivalent to the original composite, using a representative volume element (RVE). The suitable boundary conditions allow the simulation of all modes of the overall deformation arising from any arbitrary combination of mechanical and electrical loading. In the first instance, the unit cell is applied to predict the effective material coefficients of the transversely isotropic piezoelectric composite with circular cross section fibers. The numerical results are compared to other methods reported in the literature and also to results previously published, in order to evaluate the method proposal. In the second step, the method is applied to calculate the equivalent properties for smart composite materials with square cross section fibers. Results of comparison between different combinations of circular and square fiber geometries, observing the influence of the boundary conditions and arrangements are presented.

Keywords: smart composite materials, piezoelectric fiber composite, active fiber composite, finite element analyses, effective properties

Introduction

Smart composites present great potential for applications in aerospace industry. Among the alternatives to achieve such concept, there are active fiber composite (AFC) actuators developed by MIT (Bent, 1993), and macro-fiber composite (MFCTM) actuators constructed at NASA Langley Research Center (Wilkie et al., 2000). These materials have been largely investigated during the last years. Piezoelectric materials (also denoted as PZT) have the property of converting electrical energy into mechanical energy, and vice versa (Berger et al., 2005). This capability allows applications as sensors or actuators in several industrial fields, for example: noise and vibration control, acoustic speakers, precision position control and structural health monitoring (SHM). Several approaches (experimental, analytical, numerical or hybrid) have been considered to describe the electromechanical behavior of the piezoelectric coupling in composite materials. Frequently, authors apply more than one approach to obtain reliable material coefficients and electromechanical behavior evaluations (Moreno et al., 2009).

Analytical formulations to analyze and to predict of the effective electroelastic-moduli for piezoelectric composite materials are typically based on meso-mechanics, i.e. the problem consists in a piezoelectric inclusion in an infinite matrix. Chan and Unsworth (1989), as well as Smith and Auld (1991) have dealt with analytical representations, performing comparison between calculated and experimental results. Nonetheless, they were not capable of predicting the response to general loading, only for specific loading cases, because the full set of overall material parameters were determined for the specific use in medical ultrasonic imaging transducers. Dunn and Taya (1993) have employed micro-mechanical theory coupled to the electro-elastic solution and they have also studied ellipsoidal inclusions into an infinite piezoelectric medium. Rodríguez-Ramos et al. (2001) and Bravo-Castillero et al. (2001) have applied the asymptotic homogenization to composites (piezoelectric or not) with fibers in square arrangement.

Regarding numerical analyses, Finite Element Method (FEM) using the so-called Representative Volume Element (RVE)

approach (considering a unit cell) has been employed by Gaudenzi (1997) to obtain the electro-mechanical properties for piezo-composite patches applied on metallic plates. Poizat and Sester (1999) have shown how to assess two effective piezoelectric coefficients (longitudinal and transverse). Petterman and Suresh (2000) have used unit cell models applied to piezo-composites. Azzouz et al. (2001) have improved the formulation of a finite element (three nodes aniso-parametric element) to take into account the modeling of AFC and MFCTM. Paradies and Melnykowycz (2007) have studied the influence of interdigital electrodes over mechanical properties of PZT fibers. After that, the research of Kar-Gupta and Venkatesh (2005, 2007a and 2007b) have investigated the influence of fiber distribution in piezoelectric composites considering both fiber and matrix with piezoelectric properties. Berger et al. (2005 and 2006) have evaluated piezoelectric composites effective properties by comparing analytical and numerical techniques. Tan and Vu-Quoc (2005) have presented a solid-shell element formulation, only for displacement and electrical degrees of freedom, to model active composite structures considering large deformation and displacements. The authors have demonstrated the efficiency and precision in the analysis of multilayer composite structures submitted to large deformation, including piezoelectric layers. Moreno et al. (2009 and 2010) have investigated fibers with the same cross-sectional area (unimodal) and two different periodic fiber arrangements: square and hexagonal. At Moreno et al. (2010), the influence of applied boundary conditions on the determination of effective material properties for active fiber composites has been investigated.

In this paper, a method, based on FEM, is applied to determine effective properties for unidirectional periodic piezoelectric fiber composite, using individual properties of the constituent materials (fiber and matrix) and composite characteristics (e.g., geometry of the fiber or fiber volume fraction). The method proposal is based on modeling a RVE (unit cell), which is analyzed by FEM for different loadings with different boundary conditions, thereby allowing the evaluation the effective coefficients. Two case studies are considered, where in the first one, transversely isotropic piezoelectric circular fiber is adopted. The second case corresponds

to a transversely isotropic square fiber composite. It is important to note that both types of fibers are typically applied on smart composite materials, being the both cases related to AFC.

All numerical analyses have been carried out using ABAQUS™. Results are discussed, observing the influence of the boundary conditions and fiber geometries and arrangements, comparing for all combinations of circular and square cross sections in square and hexagonal arrangements.

Nomenclature

- c = elasticity tensor at constant electric field, GPa
- D = electrical displacement field, C/m^2
- e = piezoelectric coupling tensor, C/m^2
- E = electric potential field, V/m
- S = strain tensor
- T = stress tensor, N/m^2
- u = displacement, m
- V = unit cell volume, m^3
- x = coordinate
- X, Y, Z = representative volum element faces nomenclature

Greek Symbols

- ϵ = second-order dielectric tensor at constant strain field, f/m
- ϕ = electrical potential, V

Superscripts

- $\bar{}$ = medium properties
- E = constant electric field
- eff = effective properties
- n = finite element number
- S = constant strain field
- t = transpose matrix

Subscripts

- eff = effective properties
- x, y, z = coordinate system
- $1, 2, 3$ = coordinate system

Effective Properties and Representative Volume Element

In this section, the constitutive equations for electro-mechanical behavior with piezoelectric coupling for smart composite are presented. Effective properties are evaluated using homogenization method taking into account a unit cell that is a representative volume element (RVE).

Constitutive equations for smart composite material

The elastic and the dielectric behaviors are coupled in piezoelectric materials, where the mechanical stress and strain variables are related to the electric field and displacement variables. The coupling between mechanical and electric fields is obtained by piezoelectric coefficients. The constitutive equations of piezoelectric materials are assumed linear and can be written in the following matrix form:

$$\begin{Bmatrix} \{T\} \\ \{D\} \end{Bmatrix} = \begin{bmatrix} [c]^E & -[e] \\ [e]^T & [\epsilon]^S \end{bmatrix} \begin{Bmatrix} \{S\} \\ \{E\} \end{Bmatrix}, \tag{1}$$

where $\{T\}$ denotes the stress tensor, $\{S\}$ denotes the strain tensor, $\{E\}$ denotes the electric potential field, $\{D\}$ is the electrical displacement field, $[c]$ denotes fourth-order elasticity tensor at constant electric field, $[e]$ is the third-order piezoelectric coupling tensor, $[\epsilon]$ is the second-order dielectric tensor at constant strain

field, and the superscript t indicates transpose matrix, E indicates constant electric field and S constant strain field.

For an orthotropic (direction 3 aligned to the piezoelectric fibers) and transversely isotropic piezoelectric solid, the stiffness, the piezoelectric, and the dielectric matrices present 11 independent coefficients. Consequently, the constitutive relations in Eq. (1) can be written in terms of the following expanded matrix form:

$$\begin{Bmatrix} T_{11} \\ T_{22} \\ T_{33} \\ T_{12} \\ T_{23} \\ T_{31} \\ D_1 \\ D_2 \\ D_3 \end{Bmatrix} = \begin{bmatrix} c_{11}^E & c_{12}^E & c_{13}^E & 0 & 0 & 0 & 0 & 0 & -e_{13} \\ c_{12}^E & c_{11}^E & c_{13}^E & 0 & 0 & 0 & 0 & 0 & -e_{13} \\ c_{13}^E & c_{13}^E & c_{33}^E & 0 & 0 & 0 & 0 & 0 & -e_{33} \\ 0 & 0 & 0 & c_{66}^E & 0 & 0 & 0 & 0 & 0 \\ 0 & 0 & 0 & 0 & c_{44}^E & 0 & 0 & -e_{15} & 0 \\ 0 & 0 & 0 & 0 & 0 & c_{44}^E & -e_{15} & 0 & 0 \\ 0 & 0 & 0 & 0 & 0 & e_{15} & \epsilon_{11}^S & 0 & 0 \\ 0 & 0 & 0 & 0 & e_{15} & 0 & 0 & \epsilon_{11}^S & 0 \\ e_{13} & e_{13} & e_{33} & 0 & 0 & 0 & 0 & 0 & \epsilon_{33}^S \end{bmatrix} \begin{Bmatrix} S_{11} \\ S_{22} \\ S_{33} \\ S_{12} \\ S_{23} \\ S_{31} \\ E_1 \\ E_2 \\ E_3 \end{Bmatrix}. \tag{2}$$

The smart composites effective properties can be defined by the average fields in the same form as Eq. (1), which can be written in a compact matrix form, that is:

$$\begin{Bmatrix} \{\bar{T}\} \\ \{\bar{D}\} \end{Bmatrix} = \begin{bmatrix} [c]_{eff}^E & -[e]_{eff} \\ [e]_{eff}^T & [\epsilon]_{eff}^S \end{bmatrix} \begin{Bmatrix} \{\bar{S}\} \\ \{\bar{E}\} \end{Bmatrix}, \tag{3}$$

where the subscript eff denotes effective property, and $\bar{}$ average values.

The homogenization approach to a composite refers to find the functional dependence between the average variables of models that represents the coherent physical behavior. Based on the Theorem of Average with a homogenized model, mechanical and electrical properties of a unit cell, or RVE, are taken from average properties of the particular composite (Pérez-Fernandez, 2009), that is:

$$\begin{aligned} \bar{T}_{ij} &= \frac{1}{V} \int T_{ij} dV, & \bar{S}_{ij} &= \frac{1}{V} \int S_{ij} dV, \\ \bar{D}_i &= \frac{1}{V} \int D_i dV, & \bar{E}_i &= \frac{1}{V} \int E_i dV. \end{aligned} \tag{4}$$

where V is the unit cell volume and \bar{T}_{ij} , \bar{D}_i , \bar{S}_{ij} , and \bar{E}_i denote stress, electrical displacement, strain, and electric potential average values, respectively.

Using the Finite Element Method (FEM), the average values can be calculated by:

$$\begin{aligned} \bar{T}_{ij} &= \frac{1}{V} \sum_{n=1}^{nel} T_{ij}^{(n)} V^{(n)}, & \bar{S}_{ij} &= \frac{1}{V} \sum_{n=1}^{nel} S_{ij}^{(n)} V^{(n)}, \\ \bar{D}_i &= \frac{1}{V} \sum_{n=1}^{nel} D_i^{(n)} V^{(n)}, & \bar{E}_i &= \frac{1}{V} \sum_{n=1}^{nel} E_i^{(n)} V^{(n)}. \end{aligned} \tag{5}$$

where V is the volume of the unit cell, nel is the finite elements number of the complete unit cell, $V^{(n)}$ is the volume of the n^{th} element, and $T_{ij}^{(n)}$, $S_{ij}^{(n)}$, $D_i^{(n)}$ and $E_i^{(n)}$ are the respective tensors evaluated in the n^{th} element.

Representative Volume Element (RVE)

A RVE comprises the smallest portion of the composite that keeps the most representative combination of its main elements and materials. Here the RVEs are assumed as combinations of

piezoelectric fibers surrounded by a generic matrix, obeying a determined volume fraction.

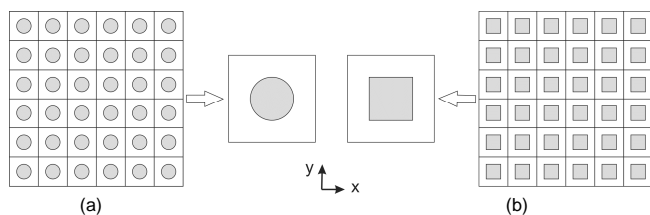


Figure 1. Smart composites arrangements of piezoelectric fibers and matrix with the corresponding unit cells used for the finite element analyses: (a) circular cross section piezoelectric fiber, and (b) square cross section piezoelectric fiber.

Figure 1 shows examples of smart composites with unidirectional piezoelectric fibers. By assuming arrangements of cubic unit cells (RVE), circular cross section (cf. Fig. 1(a), related to AFC), and square cross section (cf. Fig. 1(b), also related to AFC) represent possible geometries piezoelectric fibers in the RVE core. Moreover, in Fig. 2 one can observe details of the circular cross section RVE (square arrangement), including the representation for each of the cube faces to be used during the assessment of loading and boundary conditions. The faces location is basically related to the local reference system and denoted as X+, X-, Y+, Y-, Z+ and Z- (cf. Fig. 2). It is worth mentioning that for all further analyses in this paper, the piezoelectric fibers are considered continuous and orientated to the z-axis (or in direction 3 for coordinate system 1-2-3).

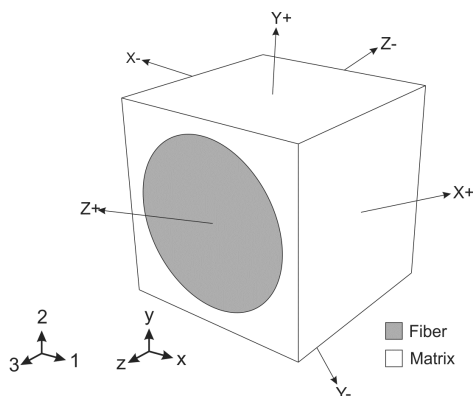


Figure 2. RVE faces nomenclature (circular cross section case).

An important aspect to be considered is the boundary conditions for the RVE assumptions. The electric-mechanical behavior is modeled by the deformation of a micro structural RVE, which reflects to its neighbor's behavior. The spatial periodicity conditions in a RVE follow from compatibility demands with respect to the opposite edges. Adjacent RVEs must have identical deformations, while neither overlapping nor separation should occur. This aforementioned compatibility condition, the so-called condition of parallelism, is illustrated by Fig. 3. Considering two points A and B, and other set of points C and D in the opposite face of a RVE (cf. Fig. 3), the displacement related to the average unit cell strain can be written as

$$u_i^A = u_i^B + \bar{S}_{ij}(x_j^A - x_j^B), \tag{6}$$

$$u_i^C = u_i^D + \bar{S}_{ij}(x_j^C - x_j^D), \tag{7}$$

where $u_i^{()}$ denotes the displacement related to the node indicated by the superscript index, \bar{S}_{ij} is the strain, and $x_j^{()}$ is the coordinate related to the node indicated by the superscript index.

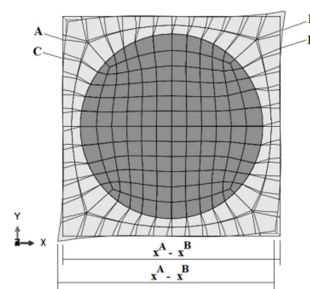


Figure 3. Condition of parallelism between opposite sides.

The same relations given in Eqs. (6) and (7) are also valid to the electrical degrees of freedom. Subtracting Eqs. (6) and (7) and considering that the average strain \bar{S}_{ij} is the same in both RVE faces, then $(x^A - x^B)$ is equal to $(x^C - x^D)$. The constraint equations for displacement and electrical potential degrees of freedom can be rewritten, respectively as

$$u_i^A - u_i^C = u_i^B - u_i^D, \tag{8}$$

$$\varphi^A - \varphi^C = \varphi^B - \varphi^D, \tag{9}$$

where $u_i^{()}$ denotes the displacement related to the node indicated by the superscript index, $\varphi_i^{()}$ is the electrical potential related to the node indicated by the superscript index.

Equations (8) and (9) represent a boundary condition of parallelism between the opposite RVE sides AC and BD. This condition must be applied for each pair of nodes in opposite sides of the unit cell (in x and y directions) and must be repeated along the z direction of the cell. However, it is not necessary to specify parallelism conditions when applying normal displacements. Regarding shear loadings, it is convenient to use an automatic procedure to search opposite nodes and apply parallelism conditions.

Finite Element Analysis

In this section, two case studies of smart composite effective properties assessment via finite element analysis approach are presented. The RVE under consideration consists of two transversely isotropic models: circular and square piezoelectric fiber.

RVE for numerical analysis

Two different unit cell configurations were used accordingly to the loading conditions and fiber arrangement. Thus square and hexagonal arrangements were applied for circular and square cross sections (cf. Figs. 4 and 5). The square arrangement was used for all loading conditions and the hexagonal arrangement was used to improve parallelism conditions representation.

In the finite element analysis, it was considered for active composite of circular cross-section fiber that the diameter is 1 mm, and for square cross-section fiber that the width is 1 mm. The fiber volume fraction is 55.5% of the unit cell total volume for both arrangements, that is, square and hexagonal, with circular or square fiber section (cf. Figs. 4 and 5).

Finite element analysis has been carried out using ABAQUS™ version 6.10 (Abaqus, 2010). Three-dimensional multi-field 20-node

quadratic piezoelectric brick elements (C3D20E-ABAQUS™ nomenclature for the element) with displacement degrees of freedom (DOF) and an additional electric potential DOF were used. These DOFs allow fully coupled electromechanical analyses.

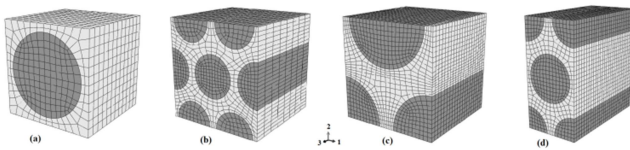


Figure 4. Finite Element Models for circular section fiber: (a) square; (b) hexagonal; (c) hexagonal (shear 1-2) and (d) hexagonal (shear 2-3).

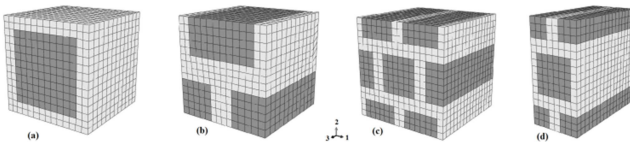


Figure 5. Finite Element Models for square section fiber: (a) square; (b) hexagonal; (c) hexagonal (shear 1-2) and (d) hexagonal (shear 2-3).

Material properties

The material properties related to the epoxy resin (composite matrix) and piezoelectric fiber (PZT-5A) were taken from Berger et al. (2005) and are shown in Table 1, according to orthotropic directions (coordinate system 1-2-3). For these analyses presented, a fiber volume fraction of 55.5% for circular section, and also, for square section fiber was adopted and the fiber is oriented in direction 3.

Table 1. Material properties for fiber and matrix.

		Fiber	Matrix
c_{11}	GPa	121.0	3.86
c_{12}		75.4	2.57
c_{13}		75.2	2.57
c_{33}		111.0	3.86
c_{44}		21.1	0.64
c_{66}		22.8	0.64
e_{13}	C/m^2	-5.4	-
e_{15}		12.3	-
e_{33}		15.8	-
ϵ_{11}	nF/m	8.11	0.0797
ϵ_{33}		7.35	0.0797

Boundary conditions

The simplified set of constitutive equations (cf. Eq. (2)), with prescribed boundary conditions allow the evaluation of the effective material properties. It is important to mention when the boundary conditions are applied in the RVE, more than one coefficient is obtained for each analysis. Therefore, to provide all eleven effective coefficients, only six analyses are necessary. More accurate results are obtained when loading is applied in fiber longitudinal direction, denoted here as z-direction (or direction 3), as well as x-direction and y-direction that are aligned with direction 1 and 2, respectively.

For the calculation of the effective coefficients c_{13}^{eff} and c_{33}^{eff} , the boundary conditions applied on the RVE have admitted normal displacements set to zero on surfaces X+, X-, Y+ and Z- ($\bar{S}_{11} = \bar{S}_{22} = \bar{S}_{12} = \bar{S}_{23} = \bar{S}_{31} = 0$), in accordance to the representation in Fig. 2.

Positive normal displacements have been prescribed on Z+ surface in z-direction ($\bar{S}_{33} \neq 0$). Electrical potentials have been set to zero on all surfaces ($\bar{E}_1 = \bar{E}_2 = \bar{E}_3 = 0$). As only \bar{S}_{33} is different from zero, first and third lines of Eq. (2) can be used to obtain:

$$c_{13}^{eff} = \bar{T}_{11} / \bar{S}_{33}, \tag{10}$$

$$c_{33}^{eff} = \bar{T}_{33} / \bar{S}_{33}. \tag{11}$$

For the calculation of the effective coefficients e_{13}^{eff} , e_{33}^{eff} and ϵ_{33}^{eff} , the RVE boundary conditions RVE have been zero for normal displacements on all surfaces ($\bar{S}_{11} = \bar{S}_{22} = \bar{S}_{33} = \bar{S}_{12} = \bar{S}_{23} = \bar{S}_{31} = 0$), also. Electrical potential have been taken as zero on z-surface with respect to the Z+ surface. Therefore, from first, third, and last lines of Eq. (2), the effective values can be obtained as:

$$e_{13}^{eff} = \bar{T}_{11} / \bar{E}_3, \tag{12}$$

$$e_{33}^{eff} = -\bar{T}_{33} / \bar{E}_3, \tag{13}$$

$$\epsilon_{33}^{eff} = \bar{D}_3 / \bar{E}_3. \tag{14}$$

The effective coefficients c_{11}^{eff} and c_{12}^{eff} have been obtained considering the RVE boundary conditions with similar conditions of those employed to the coefficients c_{13}^{eff} and c_{33}^{eff} , i.e. zero for normal displacements on surfaces X-, Y+, Y-, Z+, and Z- ($\bar{S}_{22} = \bar{S}_{33} = \bar{S}_{12} = \bar{S}_{23} = \bar{S}_{31} = 0$). Positive displacements have been prescribed on X+ surface in x-direction ($\bar{S}_{11} \neq 0$). Electrical potentials have been assumed zero on all surfaces ($\bar{E}_1 = \bar{E}_2 = \bar{E}_3 = 0$). Because only \bar{S}_{11} is different from zero, first and second lines of Eq. (2) can be used to obtain:

$$c_{11}^{eff} = \bar{T}_{11} / \bar{S}_{11}, \tag{15}$$

$$c_{12}^{eff} = \bar{T}_{22} / \bar{S}_{11}. \tag{16}$$

The effective coefficients ϵ_{11}^{eff} have been assessed with similar RVE boundary conditions of the effective coefficients e_{13}^{eff} , e_{33}^{eff} , and ϵ_{33}^{eff} , which is zero for normal displacements on all surfaces ($\bar{S}_{11} = \bar{S}_{22} = \bar{S}_{33} = \bar{S}_{12} = \bar{S}_{23} = \bar{S}_{31} = 0$). Null electrical potential on X- surface applied to the X+ surface is considered. From the seventh line in Eq. (2), the effective value of the ϵ_{11}^{eff} coefficient can be given:

$$\epsilon_{11}^{eff} = \bar{D}_1 / \bar{E}_1. \tag{17}$$

For the calculation of the effective coefficients c_{66}^{eff} , the RVE boundary conditions and loadings have admitted zero for displacements along z-direction on all nodes. All nodes located at the center line, that is perpendicular to the xy plane, had the displacements set to zero in x- and y-directions. Two opposite edges with nodes located at the cell border have been changed to cylindrical coordinate system and their displacements constrained, in order to avoid rigid body motion. Electrical potentials have been set to zero on all surfaces ($\bar{E}_1 = \bar{E}_2 = \bar{E}_3 = 0$). Shear forces with same modulus and opposite orientation have been applied on the surfaces Y+ and Y- in x-direction and on X+ and X- surfaces in y-direction, pursuing pure xy shear state. The parallelism conditions shown in Eqs. (8) and (9) must be applied between pair of surfaces X+ and X-, and between Y+ and Y- surfaces. These boundary conditions ensure the compatibility of the unit cell. As a pure shear state in xy plane has been imposed, only the component \bar{S}_{12} from

$\{\bar{S}\}$ differs from zero. These boundary conditions are illustrated in Fig. 6(a). Therefore, from the fourth line in Eq. (2), it follows

$$c_{66}^{eff} = \bar{T}_{12} / \bar{S}_{12}, \tag{18}$$

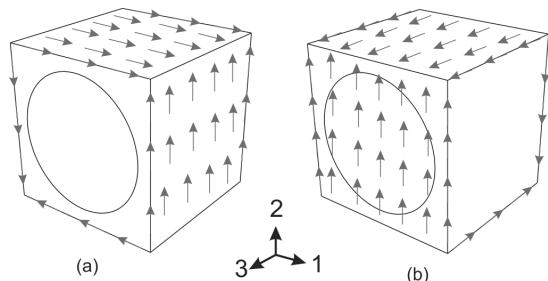


Figure 6. Boundary conditions: (a) pure shear state in xy plane; (b) pure shear state in yz plane.

Finally, for the calculation of e_{15}^{eff} and c_{44}^{eff} coefficients, the RVE boundary conditions (cf. in Fig. 6(b)) admit displacements in x-direction equal to zero for all nodes. Besides, all nodes located at the center line (perpendicular to the yz plane) present zero displacements in y- and z-directions. Similarly as in the case of the c_{66}^{eff} coefficients, the two opposite edges with nodes located at the cell border have been changed to cylindrical coordinate system and their displacements have been constrained to avoid rigid body rotation. Shear forces with same modulus and opposite orientation have been applied on the surfaces Y+ and Y- at z-direction and on

Z+ and Z- surfaces at y-direction, creating pure yz shear state. The conditions for parallelism, as shown by Eqs. (8) and (9), must be applied between pair of surfaces Z+ and Z-, and between Y+ and Y-surfaces. These boundary conditions ensure the compatibility of the unit cell. Effective coefficient ε_{11}^{eff} has been determined from Eq. (17) and effective values for e_{15}^{eff} and c_{44}^{eff} can be obtained from the fifth and eighth lines from Eq. (2), leading to:

$$e_{15}^{eff} = (-\bar{E}_2 \cdot \varepsilon_{11} + \bar{D}_2) / \bar{S}_{23}, \tag{19}$$

$$c_{44}^{eff} = (\bar{T}_{23} + \bar{E}_2 \cdot e_{15}^{eff}) / \bar{S}_{23}. \tag{20}$$

A computational procedure, based on Python language, has been developed to systematically calculate all RVE effective coefficients, thereby reducing exhaust manual work, saving time, and diminishing the chance of numerical errors. The code can also be used as template to evaluate piezoelectric fiber composites effective coefficients for arbitrary fiber volume fractions.

Results and Discussion

The effective coefficients for a piezoelectric circular cross section (PZT-5A) and epoxy resin matrix, typical for AFC arrangement, can be evaluated using results from Finite Element Analysis (FEA) and their set of equations are shown in Eq. (5). As observed in Fig. 7 and Fig. 8, it is possible to assess the numerical results to calculate the parameters required by Eq. (5).

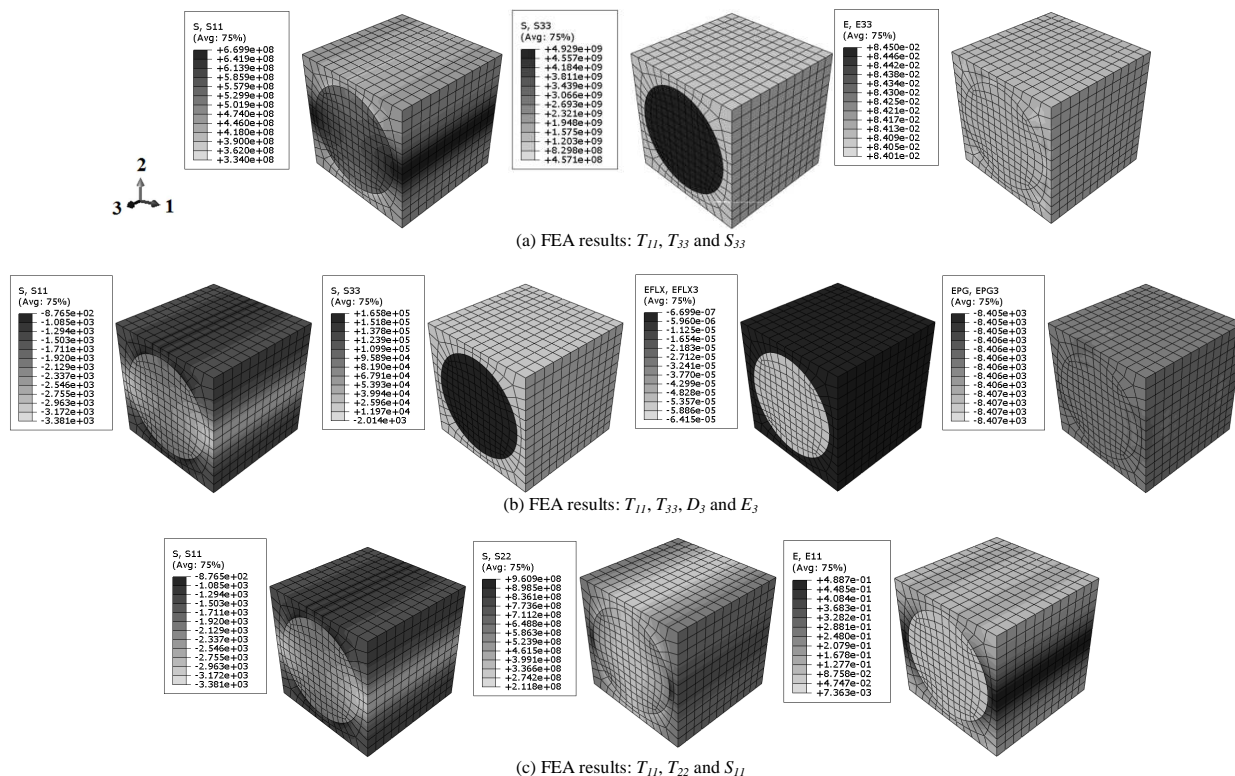


Figure 7. Square arrangement with circular geometry: non-zero average fields for 1st, 2nd and 3rd analyses.

Effective Properties Evaluation for Smart Composite Materials

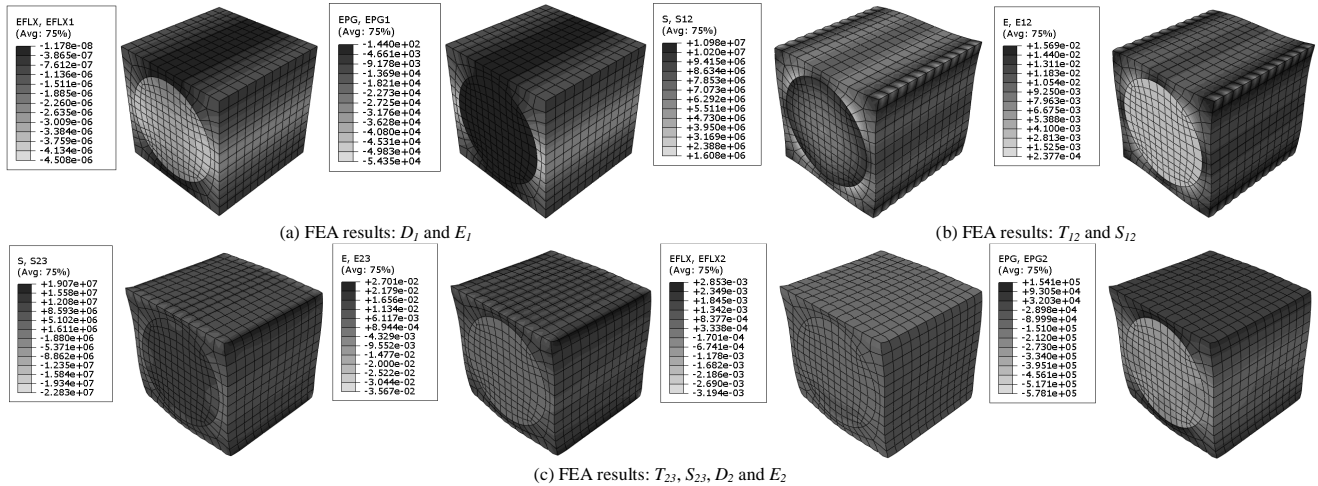


Figure 8. Square arrangement with circular geometry: non-zero average fields for 4th, 5th and 6th analyses.

It is worth remembering that all 11 effective coefficients (*cf.* Eq. (2)) have been calculated for one specific fiber volume fraction, that is, 55.5%. The method is applied and the results are compared with analytical and numerical results available in the technical literature by Berger et al. (2005) and Moreno et al. (2009), respectively. The results are summarized in Table 2. The column assigned as (1) refers to results obtained by Berger et al. (2005), while columns (2) and (3) refer to results obtained by Moreno et al. (2009). The column (1) by Berger et al. (2005) is related to analytical formulation achieved with an asymptotic homogenization method (AHM) for circular cross section. The columns (2) and (3) summarize the coefficients obtained by Moreno et al. (2009) using FEA for circular cross section with square and hexagonal unit cell arrangement, respectively.

The columns (4) and (5) summarize the effective coefficients computed by the method proposed in this work, admitting circular cross section for square and hexagonal unit cell arrangement, respectively. The effective coefficient difference values (Δ) between results are presented in the last four columns of Table 2. The first and second columns, denoting the difference values Δ_1 and Δ_2 , respectively, are taken from the analytical and numerical results presented by Berger et al. (2005) and Moreno et al. (2009) for square and hexagonal arrangements, respectively. The third and fourth columns, denoting the difference values Δ_3 and Δ_4 , respectively, are related to the analytical formulation by Berger et al. (2005) and the present work for square and hexagonal unit cell arrangements, respectively.

Table 2. Effective properties of circular cross section for square and hexagonal unit cell arrangement.

Coeff.	Units	AHM (1)	Anslys (2)	Anslys (3)	Abaqus (4)	Abaqus (5)	Δ_1 [%]	Δ_2 [%]	Δ_3 [%]	Δ_4 [%]
c_{11}^{eff}	GPa	9.5	10.88	10.68	10.856	10.356	14.53	12.42	14.27	9.01
c_{12}^{eff}		5.6	4.65	5.22	4.666	4.955	16.96	6.79	16.68	11.52
c_{13}^{eff}		6.0	6.04	6.19	6.043	6.235	0.67	3.17	0.72	3.92
c_{33}^{eff}		35.0	35.25	35.21	35.130	36.919	0.71	0.60	0.37	5.48
c_{44}^{eff}		2.2	2.15	1.95	1.969	1.905	2.27	11.36	10.50	13.41
c_{66}^{eff}		2.0	1.54	1.81	1.536	1.841	23.00	9.50	23.20	7.93
e_{13}^{eff}	C/m ²	-0.26	-0.258	-0.269	-0.2584	-0.2633	0.77	3.46	0.62	1.27
e_{15}^{eff}		0.02	0.0241	0.0164	0.0195	0.0201	20.50	18.00	2.50	0.50
e_{33}^{eff}		11.0	10.860	10.86	10.8642	11.0106	1.27	1.27	1.23	0.10
ϵ_{11}^{eff}	nF/m	0.28	0.284	0.303	0.2867	0.3026	1.43	8.21	2.39	8.07
ϵ_{33}^{eff}		4.2	4.270	4.27	4.2704	4.3222	1.67	1.67	1.68	2.91

Δ_1 - Comparing (1) and (2): Berger et al. (2005) \times Moreno et al. (2009) (Square Unit Cell)

Δ_2 - Comparing (1) and (2): Berger et al. (2005) \times Moreno et al. (2009) (Hexagonal Unit Cell)

Δ_3 - Comparing (1) and (3): Berger et al. (2005) \times Present work (Square Unit Cell)

Δ_4 - Comparing (1) and (4): Berger et al. (2005) \times Present work (Hexagonal Unit Cell)

As shown in Table 2, the effective coefficients with major difference between the analytical and numerical approach of this work have been c_{11}^{eff} , c_{12}^{eff} , c_{66}^{eff} , and e_{15}^{eff} for square cell. Similarly these differing results for those coefficients were also stated by other authors (Berger et al., 2005; Kar-Gupta and Venkatesh, 2005, 2007; Moreno et al., 2009). These coefficients are mainly influenced by the composite transversal behavior. Other influence is observed for the effective coefficients values obtained from the hexagonal cell, which can be related to the loading application. In quadratic cell, mechanical loading is applied through the epoxy resin matrix, while in the hexagonal cell arrangement it has been applied through both epoxy matrix and piezoelectric fiber.

In a hexagonal fiber arrangement, it is well known that the transverse isotropy is fully accomplished, resulting in approximate values for those found analytically. Several hypotheses can be adopted to illustrate the composites crystal symmetry, thereby creating a variety of combinations for matrix and fiber constituents

with varying degrees of anisotropy. Here, transversely isotropic piezo-fiber (poled along direction 3) and isotropic matrix (passive behavior) have been adopted, consequently the result for this combination leads to a transversely isotropic RVE behavior (poled along direction 3). Due to the crystal system tetragonal (square cell) presenting 4 mm symmetry and the crystal system hexagonal (hexagonal cell) with 6 mm symmetry, the constitutive model has shown better effective coefficient predictions for hexagonal than square cell arrangement.

On the other hand, the model is highly influenced by the applied RVE boundary conditions, due to the fact that values are in the order of Giga and Nano. For that reason, the model can be highly sensitive to changes in boundary conditions. For the remaining effective coefficients, the method applied to square and hexagonal RVE arrangements has shown adequate agreement with those presented by asymptotic homogenization method (Berger et al., 2005).

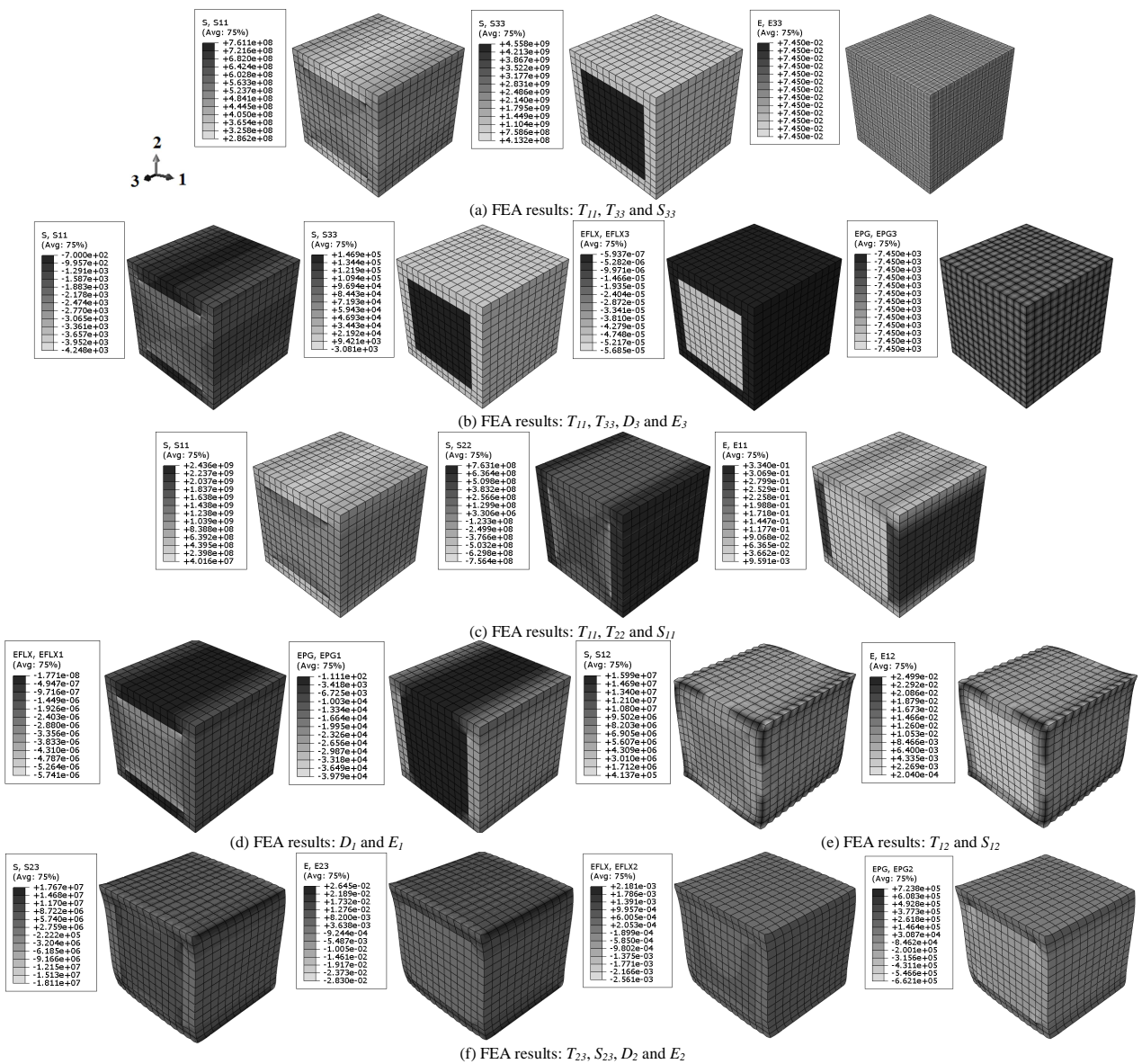


Figure 9. Square arrangement with square geometry: non-zero average fields for each analysis.

As commented earlier, present investigation has also considered other piezoelectric fiber cross-sectional geometry, that is, a square. Analogously to the previous investigation, the RVE corresponds to the piezoelectric fiber and an epoxy resin matrix with volume fiber fraction of 55.5%. Thus, all 11 effective coefficients for a square cross section can be evaluated using FEA and subsequent application of the method proposal. Figure 9 presents FEA results for aforementioned boundary conditions and respective loading described earlier.

Table 3 presents results related to the homogenized properties and comparisons between both circular and square cross sections, admitting square and hexagonal unit cells. The columns (1) to (4) present the coefficients obtained by the proposed method of this work. Differently from the previous results for circular piezoelectric fiber (cf. Table 2), here no analytical predictions have been available

to serve as comparison basis. For this reason, the comparisons have been made only for the numerical analyses as explained in this work for circular and square cross sections.

The columns (1) and (2) have the coefficients for circular cross section (square and hexagonal unit cells, respectively), while the columns (3) and (4) have effective coefficients for square cross section (also for square and hexagonal unit cells, respectively). The values attained are compared between results for circular and square piezoelectric fiber cross section, and the differences Δ_1 and Δ_2 (percentage) between these results is presented in the last two columns of Table 3. The difference Δ_1 is taken between results for circular and square cross sections, adopting square unit cell, while Δ_2 considers the difference between results for circular and square geometries, respectively, for hexagonal RVE.

Table 3. Effective properties for square cross section for square and hexagonal unit cell arrangement.

Coeff.	Units	Abaqus (1)	Abaqus (2)	Abaqus (3)	Abaqus (4)	Δ_1 [%]	Δ_2 [%]
c_{11}^{eff}	GPa	10.856	10.356	11.304	10.603	4.13	2.39
c_{12}^{eff}		4.666	4.955	4.146	4.343	11.14	12.35
c_{13}^{eff}		6.043	6.235	6.015	6.025	0.46	3.37
c_{33}^{eff}		35.130	36.919	35.106	36.573	0.07	0.94
c_{44}^{eff}		1.969	1.905	2.167	2.094	10.06	9.92
c_{66}^{eff}		1.536	1.841	1.446	1.701	5.86	7.62
e_{13}^{eff}	C/m ²	-0.2584	-0.2633	-0.2564	-0.2511	0.77	4.63
e_{15}^{eff}		0.0195	0.0201	0.0233	0.0244	19.49	21.39
e_{33}^{eff}		10.8642	11.0106	10.8657	10.9798	0.01	0.28
ϵ_{11}^{eff}	nF/m	0.2867	0.3026	0.2852	0.3158	0.52	4.36
ϵ_{33}^{eff}		4.2704	4.3222	4.2705	4.3120	0.00	0.24
Δ_1 - Comparing (1) and (3): Circular fiber cross section (square RVE) × Square fiber cross section (square RVE)							
Δ_2 - Comparing (2) and (4): Circular fiber cross section (hexagonal RVE) × Square fiber cross section (hexagonal RVE)							

As shown in Table 3, the effective coefficients for both square and hexagonal unit cells (volumetric fraction of 55.5%) have provided small difference values. However, as in previous comparisons, the c_{12}^{eff} , c_{66}^{eff} and e_{15}^{eff} coefficients have shown significant differences for both square and hexagonal unit cells, due to the aspects previously discussed for the circular cross-section piezo-fiber case (cf. Table 2). Besides, the geometries of fiber cross section are different.

Conclusions

The method proposal based on representative volume element (RVE) for predicting the homogenized properties of piezoelectric fiber composites using the finite element analysis (FEA) has shown adequate results. Longitudinal and transversal elastic and piezoelectric effective coefficients for a piezo-ceramic fiber with circular geometry embedded in a non-piezoelectric material (epoxy resin matrix) have been evaluated and compared to analytical solutions based on the asymptotic homogenization method (Berger et al., 2005). The method uses Python programming language to impose boundary conditions automatically, which speeds up considerably the calculations. This approach, however, requires particular care with RVE boundary conditions. If the boundary conditions are not applied correctly, then rigid body motions may occur and contaminate the numerical calculations. Although, great

amount of boundary conditions may lead to over constrained RVE, thereby affecting the model, also. Therefore, it is very important to balance the boundary conditions application.

In fact, numerical results in this investigation, for the square arrangement of fibers with circular geometry, have shown to be similar to those encountered in the literature. However, when comparing AFC circular and square cross-section active composites, the predicted coefficients difference values have shown that this method has appropriate convergence. These outcomes allow inferring that the method proposal is adequate to estimate effective properties for active composites.

Finally, the achievements of this investigation have also allowed concluding that the elastic transversely isotropic behavior, piezoelectric activity of the constituent phases, and influence of the relative orientation of the fiber and matrix poling directions in the hexagonal RVE arrangements provide better results when comparing with analytical ones. The reason for that can be related to the piezo-fiber crystal arrangement. Therefore, the determination of effective coefficients needs to be checked using experimental and/or other analytical analyses.

Acknowledgements

The authors are thankful to FAPESP (process number: 2009/00544-5), as well as CNPq (process number: 135652/2009-0)

and FAPEMIG for partially funding the present research work through the INCT-EIE. The authors also would like to thank Prof. Reginaldo Teixeira Coelho (EESC-USP) for the ABAQUS™ license.

References

- Abaqus, 2010, "Documentation", Version 6.10-1, Dassault Systèmes, United States of America.
- Azzouz, M.S., Mei, C., Bevan, J.S. and Ro, J.J., 2001, "Finite element modeling of MFC/AFC actuators and performance of MFC", *Journal of Intelligent Material Systems and Structures*, Vol. 12, pp. 601-612.
- Bent, A.A. and Hagood, N.W., 1993b "Development of Piezoelectric Fiber Composites for Structural Actuation," Proceeding of the 34th AIAA/ASME/ASCE/AHS Structures, Structural Dynamics and Materials Conference, April, La Jolla, CA, AIAA Paper No. 93-1717-CP pp. 3625-3638.
- Bent, A.A., 1997, "Active fiber composites for structural actuation", Thesis (PhD), Department of Aeronautics and Astronautics, Massachusetts Institute of Technology, 209 p.
- Berger, H., Kari, S., Gabbert, U., Rodriguez-Ramos, R., Guinovart, R., Otero, J.A. and Bravo-Castillero, J., 2005, "An analytical and numerical approach for calculating effective material coefficients of piezoelectric fiber composites", *International Journal of Solids and Structures*, Vol. 42, pp. 5692-5714.
- Berger, H., Kari, S., Gabbert, U., Rodriguez-Ramos, R., Bravo-Castillero, J., Guinovart-Diaz, R., Sabina, F.J. and Maugin, G.A., 2006, "Unit cell models of piezoelectric fiber composites for numerical and analytical calculation of effective properties", *Smart Materials and Structures*, Vol. 15, pp. 451-458.
- Bravo-Castillero, J., Guinovart-Diaz, R., Sabina, F.J. and Rodríguez-Ramos, R., 2001, "Closed form expressions for the effective coefficients of a fiber-reinforced composite with transversely isotropic constituents – II. Piezoelectric and square symmetry", *Mechanics of Materials*, Vol. 33, pp. 237-248.
- Chan, H.L.W. and Unsworth, J., 1989, "Simple model for piezoelectric ceramic/polymer 1-3 composites used in ultrasonic transducer applications", *IEEE Transactions on Ultrasonics, Ferroelectrics and Frequency Control*, Vol. 36, pp. 434-441.
- Dunn, M.L. and Taya, M., 1993, "Micromechanics predictions of the effective electroelastic moduli of piezoelectric composites", *International Journal of Solids and Structures*, Vol. 30, pp. 161-175.
- Gaudenzi, P., 1997, "On the electro mechanical response of active composite materials with piezoelectric inclusions", *Computers & Structures*, Vol. 65, pp. 157-168.
- Kar-Gupta, R. and Venkatesh, T.A., 2005, "Electromechanical response of 1-3 piezoelectric composites: effect of poling characteristics", *Journal of Applied Physics*, Vol. 98, 14 p.
- Kar-Gupta, R. and Venkatesh, T.A., 2007, "Electromechanical response of 1-3 piezoelectric composites: a numerical model to assess the effects of fiber distribution", *Acta Materialia*, Vol. 55, pp. 1275-1292.
- Moreno, M.E., Tita, V. and Marques, F.D., 2009, "Finite element analysis applied to evaluation of effective material coefficients for piezoelectric fiber composites", in 2009 Brazilian Symposium on Aerospace Eng. & Applications, September 14-16, 2009, S. J. Campos, SP, Brazil.
- Moreno, M.E., Tita, V. and Marques, F.D., 2010, "Influence of boundary conditions on the determination of effective material properties for active fiber composites", in 2010 Pan-American Congress of Applied Mechanics, January 04-08, 2010, Foz do Iguacu, PR, Brazil.
- Paradies, R. and Melnykowycz, M., 2007, "Numerical stress investigation for piezoelectric elements with circular cross section and interdigitated electrodes", *Journal of Intelligent Material Systems and Structures*, Vol. 18, pp. 963-972.
- Pérez-Fernandez, D., 2009, "Un enfoque integrador de métodos asintóticos y variacionales para la evaluación del comportamiento efectivo de materiales compuestos magneto-electro-elásticos no lineales provistos de una estructura periódica.", Tesis (Doctor en Ciencias Matemáticas) – Instituto de Cibernética, Matemática y Física, Departamento de Física Aplicada, La Habana, Cuba.
- Pettermann, H.E. and Suresh, S., 2000, "A comprehensive unit cell model: a study of coupled effects in piezoelectric 1-3 composites", *International Journal of Solids and Structures*, Vol. 37, pp. 5447-5464.
- Piezoelectric Ceramic for Sonar Transducers (Hydrophones & Projectors) Military Standard US DOD MIL STD 1376 A (SH) (1984).
- Poizat, C. and Sester, M., 1999, "Effective properties of composites with embedded piezoelectric fibres", *Computational Materials Science*, Vol. 16, pp. 89-97.
- Rodríguez-Ramos, R., Sabina, F.J., Guinovart-Díaz, R. and Bravo-Castillero, J., 2001, "Closed form expressions for the effective coefficients of a fiber-reinforced composite with transversely isotropic constituents – I. Elastic and square symmetry", *Mechanics of Materials*, Vol. 33, pp. 223-235.
- Smith, W.A. and Auld, B.A., 1991, "Modeling 1-3 composite-piezoelectrics: thickness-mode oscillations", *IEEE Transactions on Ultrasonics, Ferroelectrics and Frequency Control*, Vol. 38, pp. 40-47.
- Tan, X.G. and Vu-Quoc, L., 2005, "Optimal solid shell element for large deformable composite structures with piezoelectric layers and active vibration control", *International Journal for Numerical Methods in Engineering*, Vol. 64, pp. 1981-2013.
- Wilkie, W.K., High, J.W., Mirick, P.H., Fox, R.L., Little, B.D., Bryant, R.G., Hellbaum, R.F., Jalink, A., Jr., 2000, "Low-Cost Piezocomposite Actuator for Structural Control Applications," in Industrial and Commercial Applications of Smart Structures Technologies, SPIE 7th International Symposium on Smart Structures and Materials, March 5-9, 2000 Newport Beach, California.